This is an open access article published under an ACS AuthorChoice License, which permits copying and redistribution of the article or any adaptations for non-commercial purposes.

ACS central science

Research Article

Cite This: ACS Cent. Sci. 2019, 5, 1179−1186

http://pubs.acs.org/journal/acscii

Electrochemical Reoxidation Enables Continuous Methane-to-Methanol Catalysis with Aqueous Pt Salts

R. Soyoung Kim and Yogesh Surendranath*

Department of Chemistry, Massachusetts Institute of Technology, Cambridge, Massachusetts 02139, United States

Supporting Information

ABSTRACT: The direct conversion of methane to methanol would enable better utilization of abundant natural gas resources. In the presence of stoichiometric Pt^{IV} oxidants, Pt^{II} ions are capable of catalyzing this reaction in aqueous solutions at modest temperatures. Practical implementation of this chemistry requires a viable strategy for replacing or regenerating the expensive Pt^{IV} oxidant. Herein, we establish an electrochemical strategy for continuous regeneration of the Pt^{IV} oxidant to furnish overall electrochemical methane oxidation. We show that Cl-adsorbed Pt electrodes catalyze facile oxidation of Pt^{II} to Pt^{IV} at low overpotential without concomitant methanol oxidation. Exploiting this facile electrochemistry, we maintain the $Pt^{II/IV}$ ratio during Pt^{II}-catalyzed methane oxidation via in situ monitoring of the solution potential coupled with dynamic modulation of the electric current. This approach leads to sustained methane oxidation catalysis with 70% selectivity for methanol.

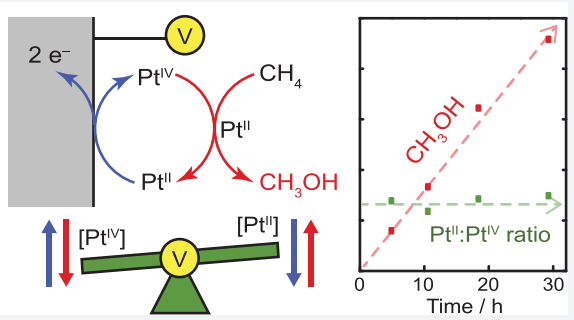

INTRODUCTION

Methane is an abundant hydrocarbon resource that is often underutilized because of its low boiling point and chemical inertness. Thus, technologies for converting methane to high-demand liquid chemicals such as methanol would enable better utilization of this low-carbon resource.[1−3] Current methane valorization technologies rely on an indirect process involving initial steam reforming to H_2 and CO. The reforming step requires capital-intensive facilities that are not amenable to remote deployment.[4] Consequently, spontaneously released natural gas at oil wells is being flared at massive scales.[5,6] The development of mild, direct methane-to-methanol processes (eq 1) that can operate portably is expected to stem flaring as well as expand the versatility of natural gas.[7,8]

$$CH_4 + 0.5\ O_2 \rightarrow CH_3OH \quad (1)$$

While many homogeneous and heterogeneous systems have been investigated for methane-to-methanol conversion,[1,8] simple Pt^{II} chloride salts in water, $Pt^{II}Cl_x(H_2O)_{(4-x)}^{(2-x)}$ (denoted collectively as Pt^{II}), offer unique advantages.[9] The catalytic cycle (Scheme 1) is initiated by Pt^{II} ions, which carry out reversible C−H activation of CH_4 to yield a $Pt^{II}-CH_3$ intermediate. This intermediate is then oxidized by $Pt^{IV}Cl_x(H_2O)_{(6-x)}^{(4-x)}$ (denoted collectively as Pt^{IV}) to generate a $Pt^{IV}-CH_3$ species that undergoes rapid reductive elimination to produce CH_3OH or CH_3Cl, which can be hydrolyzed to CH_3OH. This system has the following advantages: First, the organometallic activation of methane offers superior selectivity for mono-oxidation compared to catalysts that operate via radical intermediates.[8,10−12] Second, while most homogeneous catalysts that do organometallic activation require impractical[8,13] concentrated acid media for boosting the catalytic rate and selectivity,[14,15] Pt^{II} operates in dilute aqueous acids. Along with the relatively low reaction temperature (>100 °C), these advantages position Pt^{II} chloride salts, often referred to as "Shilov's catalyst," as privileged agents for methane-to-methanol conversion under mild conditions.

Scheme 1. Catalytic Cycle for the Functionalization of Methane by Aqueous Pt Salts (Shilov's Catalyst) and Distinct Strategies To Overcome the Stoichiometric Use of Pt^{IV}

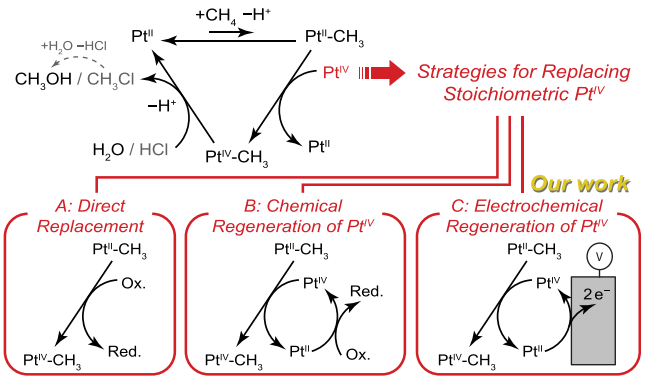

A critical drawback of Shilov's catalyst, as originally reported, is its requirement for a stoichiometric Pt^{IV} oxidant, which is economically impracticable.[9] The key to developing an alternative oxidation strategy for this catalytic system is to

Received: March 18, 2019
Published: June 17, 2019

© 2019 American Chemical Society

DOI: 10.1021/acscentsci.9b00273
ACS Cent. Sci. 2019, 5, 1179−1186

achieve precise control over the driving force (thermodynamics) and/or rate (kinetics) of the oxidation reaction. In view of the catalytic cycle, there are two distinct approaches to the problem. First, Pt^{IV} may be directly replaced by an alternative oxidant that can oxidize the $Pt^{II}-CH_3$ intermediate (Scheme 1, Strategy A). Success of this strategy requires an oxidant that (i) rapidly oxidizes the fleeting $Pt^{II}-CH_3$ intermediate before it can undergo protonation back to Pt^{II} + CH_4 and (ii) possesses a low enough redox potential to avoid oxidizing the Pt^{II} catalyst to Pt^{IV}, which is unreactive toward CH_4. The conflicting requirement for fast rates and low driving force places an inherent constraint on the oxidants that are viable. Second, one may employ Pt^{IV} itself, which is an efficient oxidant for $Pt^{II}-CH_3$, as a redox mediator for the overall reaction (Scheme 1, Strategy B). Success of this strategy hinges on carefully matching the rate of Pt^{IV} regeneration by Pt^{II} oxidation to the rate of Pt^{IV} consumption by methane functionalization. Rapid Pt^{II} oxidation will progressively deplete the pool of Pt^{II}, retarding catalysis, whereas slow oxidation will deplete Pt^{IV} and induce irreversible decomposition of the Pt^{II} to metallic Pt^0 via, inter alia, disproportionation of Pt^{II}.[9,16] Thus, a viable alternate oxidant must achieve good control over the oxidation driving force and/or rate.

The inherent difficulty of fine-tuning oxidation using chemical reagents has, presumably, contributed to the limited success in replacing stoichiometric Pt^{IV}. Notably, oxidants such as heteropoly acids, $CuCl_2$, $FeCl_3$, and Br_2 were identified as kinetically competent toward the oxidation of $Pt^{II}-CH_3$ (Scheme 1, Strategy A).[17] These oxidants have achieved Pt^{II}-mediated oxidation of methane or other aliphatic substrates,[18−21] and some of them, being air-regenerable, have been employed in concert with O_2 to effect overall aerobic methane functionalization. However, none of these studies established long-term stability. For example, the combination of $CuCl_2$ and O_2 ultimately resulted in complete oxidation of Pt^{II} to Pt^{IV},[9] highlighting the difficulty of controlling the oxidation driving force. Studies aimed at mediating turnover via the $Pt^{II/IV}$ redox couple (Scheme 1, Strategy B) showed that Cl_2[22] and H_2O_2[16] are viable oxidants. However, the Pt^{II} oxidation rate was not actively modulated, and thus, continuous operation was not demonstrated. Furthermore, neither of these oxidants are air-regenerable or affordable for methanol production. In sum, there exists yet no suitable alternative to stoichiometric Pt^{IV} for sustained aqueous Pt^{II}-catalyzed methane-to-methanol conversion.

We show that electrochemistry affords a unique solution to this problem. Unlike all stoichiometric chemical oxidations, electrochemical oxidation allows for unparalleled control over the rate and driving force for electron transfer. Furthermore, the rate and driving force can be toggled instantaneously for real-time, dynamic modulation. While direct electro-oxidation of the fleeting $Pt^{II}-CH_3$ intermediate is unfeasible due to the small fraction of reaction solution volume in contact with the electrode surface, electrochemistry is well-suited to regenerate Pt^{IV} via reoxidation of Pt^{II} (Scheme 1, Strategy C). As noted above, the success of this approach relies on maintaining a constant Pt^{II}:Pt^{IV} ratio; electrochemistry allows for simultaneous measurement and fine-tuning of this ratio in real-time. In addition, coupling the methane oxidation half-reaction with an oxygen reducing cathode would render the overall process aerobic (eq 1).

Despite its attractiveness, there exist a paucity of examples of this approach. One report applied electrochemical oxidation in the presence of Pt^{II}, heteropoly acids, and O_2 to achieve 1.4 turnovers for methanol production, but no information about the mechanism or stability of the system was provided.[23] Earlier, a similar scheme was employed to oxidize a test substrate, *p*-toluenesulfonic acid; while 11 turnovers of the Pt^{II} catalyst were attained, deposition of Pt^0 was observed with increasing reaction times.[24] A particular impediment to electrochemical turnover of the aqueous Pt^{II} catalyst is the general sluggishness of two-electron $Pt^{II/IV}$ oxidation at an electrode.[25,26] Previously, we used electrochemical oxidation of Pd^{II} salts to generate a highly electrophilic $Pd_2^{III,III}$ species that effects methane conversion to methanol precursors.[27] While this system showed exceptional rates and high selectivity, it required concentrated acid media that restrict practical utility. Herein, we combine Pt electrodes that catalyze facile electrochemical oxidation of Pt^{II} to Pt^{IV} ions[28] with in situ modulation of electric current to achieve continuous, steady-state methane oxidation over the course of 30 h. We observe the generation of methanol and methyl chloride as the principal products with >80% combined selectivity, demonstrating continuous Pt^{II}-catalyzed electrochemical methane oxidation.

RESULTS AND DISCUSSIONS

Identification of a Suitable Electrode for the Pt^{II}-Catalyzed Electrochemical Methane Oxidation Reaction (EMOR). The electrochemical mediation scheme put forward above (Scheme 1, Strategy C) requires an electrode capable of oxidizing Pt^{II} to Pt^{IV}. In view of the high $Pt^{II/IV}$ oxidation potential (E^0 = 0.68 V versus SHE for $Pt^{II}Cl_4^{2-}/Pt^{IV}Cl_6^{2-}$)[29] and the acidic environment required for stability of the Pt ions,[30] we focused our investigations on carbon, fluorine-doped tin oxide (FTO), and Pt electrodes as possible candidates. Whereas carbon and FTO electrodes displayed progressive deactivation and/or sluggish Pt^{II} oxidation kinetics (see the SI, Section S2), Pt electrodes showed facile oxidation of Pt^{II} at modest potentials. In 0.5 M H_2SO_4, the Pt electrode displays the typical voltammetric features associated with hydrogen underpotential deposition (H UPD) and oxide formation at low and high potentials, respectively (Figure 1a, black; also Figure S1).[31,32]

Upon addition of 1 mM $Pt^{II}Cl_4^{2-}$, a reversible wave appears at $E_{p,a}$ = 1.1 V and $E_{p,c}$ = 0.8 V (Figure 1a, blue). The appearance of this wave is accompanied by a suppression in the background Pt oxide wave, which we ascribe to inhibition by surface-adsorbed Cl^- that has dissociated from the $Pt^{II}Cl_4^{2-}$ ions (Figure S14).[33] As sustained methanol production requires Cl^- ions (see below), we also examined the voltammetric response of Pt^{II} in the presence of 10 mM Cl^- (Figure 1a, red). Whereas the Pt^{II} oxidation wave is largely unaffected by the additional Cl^-, the cathodic wave associated with Pt^{IV} back-reduction is significantly suppressed. These observations are in line with the previous literature on $Pt^{II/IV}$ oxidation at Pt electrodes that invokes an inner-sphere electron transfer mechanism involving transfer of a surface-adsorbed Cl^- to Pt^{II} during the oxidation reaction.[28] Indeed, the reported Cl-adsorption isotherm at 2 mM Cl^- stretches from 0 to 0.8 V versus SHE (Figure S15),[34] showing near-saturation at the potential for Pt^{IV} reduction. These observations suggest that Cl^- surface coverage at this potential may be incomplete at low [Cl^-] but complete at 10 mM Cl^-. Thus, higher surface

DOI: 10.1021/acscentsci.9b00273
ACS Cent. Sci. 2019, 5, 1179−1186

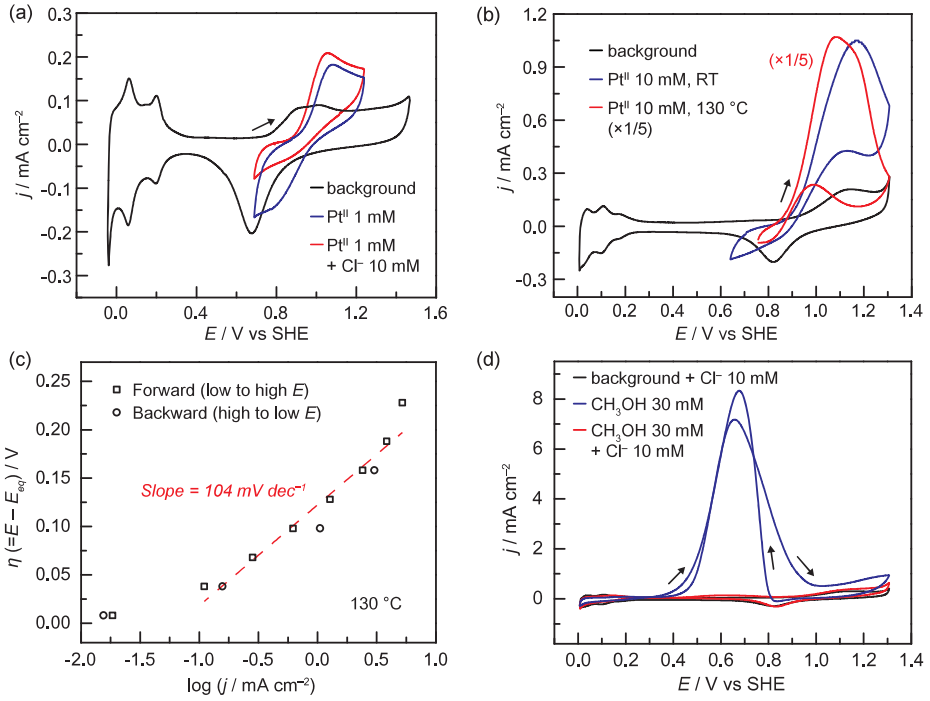

Figure 1. (a) Cyclic voltammograms obtained on a Pt disk electrode at room temperature in 0.5 M H_2SO_4; (black) background, (blue) 1 mM $K_2Pt^{II}Cl_4$, and (red) 1 mM $K_2Pt^{II}Cl_4$ with 10 mM NaCl. (b) Cyclic voltammograms obtained on a Pt wire electrode in 10 mM NaCl, 0.5 M H_2SO_4; (black) background, (blue) 10 mM $K_2Pt^{II}Cl_4$ at room temperature, and (red) 10 mM $K_2Pt^{II}Cl_4$ at 130 °C. (c) Tafel plot at 130 °C for Pt^{II} electro-oxidation. The solution contained 5 mM each of $K_2Pt^{II}Cl_4$ and $Na_2Pt^{IV}Cl_6$ in 10 mM NaCl, 0.5 M H_2SO_4. E_{eq} (= 0.829 V vs SHE) was obtained from the open-circuit potential. (d) Cyclic voltammograms obtained on a Pt wire electrode in 10 mM NaCl, 0.5 M H_2SO_4 at 130 °C; (black) background, (blue) 30 mM CH_3OH without the 10 mM NaCl, and (red) 30 mM CH_3OH. All scan rates = 100 mV s^{-1}.

coverage of Cl^- induced by higher [Cl^-] has a negligible impact on Pt^{II} oxidation, but the back-reduction of Pt^{IV}, which requires Cl^- transfer back to the electrode surface, is inhibited (see the SI, Section S2, for additional explanation). This inner-sphere mechanism explains why Pt electrodes display superior Pt^{II} electro-oxidation kinetics compared to carbon or FTO.

Having identified a suitable electrode material, we then investigated $Pt^{II/IV}$ electro-oxidation at the elevated temperatures required for methane activation by Pt^{II}. These experiments were conducted above the boiling point of water and were, therefore, carried out in a home-built high-pressure electrochemical cell (see the SI and below). As shown in Figure 1b, red, high Pt^{II} oxidation current flowed at 130 °C; the 5-fold enhancement in current and approximately 100 mV negative shift in $E_{p,a}$ compared to room temperature (Figure 1b, blue) reflect faster mass transport and electrode kinetics. The decrease in current at E > 1.1 V is attributed to the formation of surface oxides that inhibit the inner-sphere Pt^{II} oxidation. This inhibition is particularly pronounced at high [Pt^{II}] and high temperatures (see the SI, Section S2, for details). We also examined the dependence of Pt^{II} oxidation current on electrochemical driving force (Figure 1c). Keeping the potential below Pt oxide formation, <1.1 V, the steady-state current increased 10-fold per 104 mV of additional overpotential ($\eta = E - E_{eq}$). This Tafel slope at 130 °C corresponds to a rate-limiting one-electron transfer with a transfer coefficient of 0.77, in agreement with the aforementioned mechanism.[35] These results show that Pt electrodes are capable of facile oxidation of Pt^{II} at elevated temperatures.

Pt electrodes were also capable of sustained and efficient $Pt^{II/IV}$ oxidation. We carried out bulk electrolyses of a stirred solution at 130 °C by applying a constant potential below 1.1 V. After chronoamperometry at 0.874, 0.924, and 0.974 V for 77, 40, and 17 min, respectively, half of the Pt^{II} ions in the initial solution were converted to Pt^{IV} ions as determined by UV−Vis analysis. At all three potentials examined, Pt^{IV} was generated with 100% Faradaic efficiency (Table S1).

Sustained methane oxidation catalysis will lead to a progressive rise in methanol concentration in the reactor over time. Thus, in addition to supporting facile $Pt^{II/IV}$ oxidation, the electrode must be inert toward further oxidation of the CH_3OH product. This is a particular concern for Pt, which is the standard electrocatalyst for oxidation of CH_3OH to CO_2.[36] Indeed, in 0.5 M H_2SO_4 at 130 °C, addition of 30 mM CH_3OH gives rise to the well-known anodic features associated with CH_3OH electro-oxidation (Figure 1d, blue).[37] Remarkably, upon addition of 10 mM Cl^-, this CH_3OH oxidation feature is almost completely suppressed (Figure 1d, red) over the entire potential range examined. This suppression is ascribed to surface adsorption of Cl^- ions.[38] An additional control experiment confirmed that the non-electrochemical oxidation of CH_3OH catalyzed on metallic Pt[39] is also negligible under our conditions (see the SI, Section S2). These data indicate that, fortuitously, the presence of Cl^- serves to simultaneously promote $Pt^{II/IV}$ oxidation and suppress surface-catalyzed oxidation of the methanol product. Together, these studies establish that Pt electrodes are suitable for EMOR.

Sustained Methane Oxidation Catalysis via Dynamic Electrochemical Control of the Pt^{II}:Pt^{IV} Ratio. The above studies provide the basis for carrying out continuous methane-to-methanol oxidation catalysis via electrochemical regeneration of Pt^{IV} (Scheme 1, Strategy C). The EMOR was carried out in a home-built high-pressure cell which consisted of a

DOI: 10.1021/acscentsci.9b00273
ACS Cent. Sci. 2019, 5, 1179−1186

modified Parr reactor with electrical feedthroughs (Figure 2; see the SI, Section S1, for full details). The working

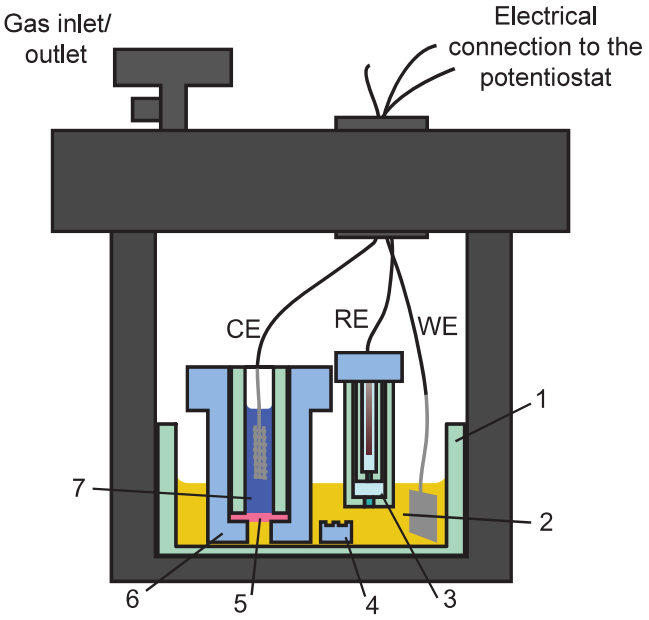

Figure 2. High-pressure, three-electrode, two-compartment electrochemical cell for the EMOR. WE, Pt foil working electrode; RE, Ag/AgCl reference electrode; CE, Pt mesh counter electrode. 1, glass cell; 2, working solution containing the Pt ions; 3, fritted tubes for housing the RE; 4, PTFE stir bar; 5, H^+-conducting membrane separating the counter compartment; 6, PTFE body holding the membrane stack; 7, counter compartment solution containing $(V^{IV}O)(SO_4)$ as the sacrificial electron acceptor.

compartment was charged with 3 mM Pt^{II} and 7 mM Pt^{IV} in 10 mM NaCl, 0.5 M H_2SO_4 (see the SI, Section S4, for details of electrolyte optimization). The counter compartment, separated by a H^+-conducting membrane stack, contained 3 M vanadyl sulfate ($(V^{IV}O)(SO_4)$) as a sacrificial oxidant to be reduced at the cathode. In a practical device, oxygen could be supplied to the cathode, but given the low solubility of O_2 and complications of co-pressurizing the cell with O_2, we opted to use the vanadyl ion as a surrogate. The highly soluble and fairly inert vanadyl ions enabled examination of long-term electrolysis. This counter reaction prevented H_2 evolution, which must be avoided in this configuration due to the irreversible reduction of Pt^{II} to Pt^0 by H_2; however, in a well-engineered system with good gas stream separation, H_2 may be deliberately generated as a useful byproduct. The solutions and the cell were purged to remove O_2 prior to pressurization with 500 psi of methane. Following heating and temperature stabilization at 130 °C, electrolysis was initiated to continuously reoxidize Pt^{II} during methane functionalization catalysis. The electrolysis was carried out with control of the current instead of the potential, which is the preferred method in industrial electrolysis.[40]

Careful choice of the applied current is critical for sustained catalysis. To maintain a constant Pt^{II}:Pt^{IV} ratio over the course of the reaction, the rate of Pt^{II} oxidation at the electrode must match the rate of methane oxidation catalysis in the solution. A simple mathematical derivation shows that, at a fixed rate of $Pt^{II/IV}$ oxidation, any small difference between the two rates will cause the Pt^{II}:Pt^{IV} ratio to deviate from the initial value exponentially over time (SI, Section S6). Thus, the applied current must be constantly readjusted to match the rate of catalysis to maintain a steady ratio of Pt^{II}:Pt^{IV}. To achieve this, we employed the open-circuit potential (OCP) of the working compartment as an in situ probe of the instantaneous Pt^{II}:Pt^{IV} ratio in solution and adjusted the current (i) accordingly. In our reactor, the Pt^{II} and Pt^{IV} ions exist in various ligated states ($Pt^{II}Cl_x(H_2O)_{(4-x)}^{(2-x)}$ and $Pt^{IV}Cl_x(H_2O)_{(6-x)}^{(4-x)}$), each pair of which has different redox potentials. Assuming that $[Cl^-]$ is constant, the following modified form of the Nernst equation may be derived:

$$E = E^C + \frac{RT}{2F}\ln\frac{[Pt^{IV}]}{[Pt^{II}]}; \quad E^C = E^{0\prime\prime} + \frac{RT}{2F}\ln\frac{1}{[Cl^-]^n} \tag{2}$$

where $E^{0\prime\prime}$ and n represent the weighted average of the redox potentials and Cl^- stoichiometries, respectively. Thus, using eq 2, we can estimate the instantaneous Pt^{II}:Pt^{IV} ratios potentiometrically. E^C can be determined from the initial OCP reading and the known initial Pt^{II}:Pt^{IV} ratio.

Figure 3 shows the electrochemical data recorded during a typical EMOR trial with periodic OCP monitoring and

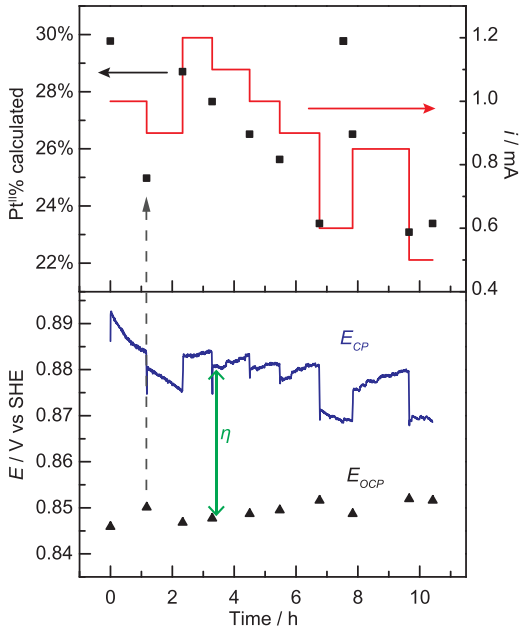

Figure 3. Representative electrochemical data recorded during an EMOR trial (the 10.5 h long trial in Table 1). The open-circuit potential (E_{OCP}) reading at approximately 1 h time intervals (bottom, black triangles) was used to calculate the Pt^{II}% in the solution (top, black squares). This was in turn used to determine how much current to pass (top, red line), and the electrode potential during the electrolysis (E_{CP}) was recorded (bottom, blue line).

adjustment of the current. To aid the interpretation, the Pt^{II}:Pt^{IV} ratio was converted to the percentage of Pt^{II} ions (Pt^{II}%), defined as $[Pt^{II}]/([Pt^{II}] + [Pt^{IV}])$. In a representative reaction, after 1.0 mA of current was passed for 1 h, the Pt^{II}% decreased from 30% to 25%. This led us to adjust the current to 0.9 mA, and after another 1 h, the Pt^{II}% rose to 29%. This process of quantifying the Pt^{II}% in the solution and adjusting the current to maintain a roughly constant Pt^{II}% was repeated periodically until the reaction was terminated. Incidentally, while our test reactor was too congested to conveniently add a fourth electrode, incorporation of a separate sensing electrode

DOI: 10.1021/acscentsci.9b00273
ACS Cent. Sci. 2019, 5, 1179−1186

Table 1. Results of EMOR Trials at T = 130 °C and P_{CH_4} = 675 psi[a]

				product [μmol (relative fraction)]					approximate TON[b]		approximate TOF[b] (h^{-1})	
time[c] (h)	i_{ave}[d] (mA)	ΔOCP[e] (mV)	final [Pt^{II}%]	CH_3OH	CH_3Cl	$CH_2(OH)_2$[f]	HCOOH	CO_2	CH_3X	total	CH_3X	total
4.9	1.19	7.9	22%	60.5 (72%)	20.1 (24%)	2.2 (3%)	0.1 (0%)	1.1 (1%)	1.4	1.6	0.29	0.32
10.5	0.88	5.7	19%	93.7 (71%)	27.9 (21%)	5.1 (4%)	1.2 (1%)	4.4 (3%)	2.3	2.9	0.21	0.27
18.4	1.00	−2.8	22%	205.4 (72%)	44.8 (16%)	21.9 (8%)	2.9 (1%)	12.2 (4%)	4.5	6.3	0.24	0.34
29.3	0.91	−6.0	23%	268.0 (69%)	52.0 (13%)	36.4 (9%)	7.2 (2%)	24.1 (6%)	5.8	9.3	0.20	0.32

[a]Initial [Pt^{II}] and [Pt^{IV}] in the working solution were 3 mM and 7 mM, respectively, and the solution volume was 23 mL. The electrochemically active surface area of the Pt working electrode was 10.3 cm^2. [b]The TONs were determined from dividing the moles of product by the average of the initial and final moles of Pt^{II} for each reaction. The TOFs were obtained by dividing the TON by the time duration of each reaction. The total number of turnovers was calculated by assuming that all oxidation reactions were catalyzed by Pt^{II}: ($\mu mol_{CH_3OH} + \mu mol_{CH_3Cl} + 2 \times \mu mol_{CH_2(OH)_2} + 3 \times \mu mol_{HCOOH} + 4 \times \mu mol_{CO_2}$) was divided by the average $\mu mol_{Pt^{II}}$ to determine total TON. For CH_3X-specific turnovers, only ($\mu mol_{CH_3OH} + \mu mol_{CH_3Cl}$) was divided by $\mu mol_{Pt^{II}}$. [c]The reaction time is the length of time the reactor was at the designated temperature, which spanned from ∼80 min after the start of heating to the time at which the reactor was removed from the oil bath. [d]i_{ave} was calculated by dividing the total charge passed by the reaction time. [e]ΔOCP is the difference between the first and last OCP readings (= $OCP_{last} - OCP_{first}$). [f]The hydrated form of formaldehyde, which is the predominant form of formaldehyde in the acidic pH employed.

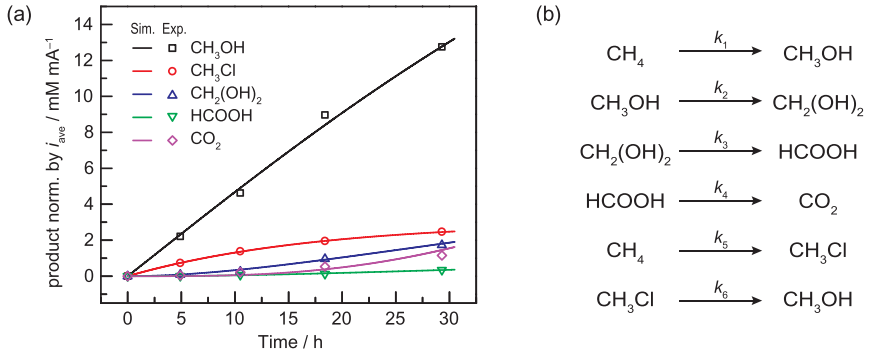

Figure 4. (a) Amounts of methane oxidation products generated in the EMOR reactor versus reaction time. Each point represents a different trial in Table 1, and the product concentrations were normalized by i_{ave} of each trial (see the SI, Section S6, for explanation). The lines represent fitting with the (b) set of putative reactions.

could allow, in principle, for real-time feedback modulation of i.

The potential required for electrolysis (E_{CP}, CP = chronopotentiometry) equals the equilibrium electrode potential (E_{OCP}) plus the magnitude of overpotential (η) applied. By definition, η is the difference between the applied potential (E_{CP}) and E_{OCP}, as marked with green arrows in Figure 3. Over multiple trials, we consistently observed a steady decrease in η during the initial 2−3 h of each electrolysis, which we attribute to a slow initial electrode activation process. After stabilization of the electrode activity, η was ca. 20−40 mV, at an average current of around 0.9 mA. Normalizing by the electrode surface area, we estimate an average current density of 0.09 mA cm^{-2}. This is in line with the previously obtained Tafel plot (Figure 1c) after considering the difference in [Pt^{II}] (5 mM in the Tafel plot, approximately 3 mM in the EMOR trials). While the required η in our system is an extrinsic parameter that depends on the reactor configuration (see the SI, Section S6), we emphasize that the fast Pt^{II} oxidation kinetics on the Pt electrode enable such a low η.

Independent quantification of the Pt^{II}:Pt^{IV} ratio at the end of the EMOR experiment confirmed the power of in situ current modulation. At the end of each reactor trial, [Pt^{II}] and [Pt^{IV}] in the working compartment were measured by UV−Vis spectroscopy. Despite a wide variation in reaction time (5−29 h) and consequently turnover number (see below), UV−Vis analysis confirmed that the final Pt^{II}% (19−23%) values were all similar (Table 1). These values are somewhat lower than the initial Pt^{II}% (30%), reflecting our preference to err on the side of lower Pt^{II}% to prevent irreversible Pt^0 deposition (see below). Interestingly, despite the agreement in final Pt^{II}% values, ΔOCP (= $OCP_{last} - OCP_{first}$), which should reflect the final Pt^{II}% according to eq 2, was more negative for longer reactions by up to 14 mV. We postulate that this may be due to decreasing [Cl^-] in the reaction solution as a result of CH_3Cl formation. Despite this additional long-term effect, changes in the OCP between constant-current intervals provided a faithful indication of whether the Pt^{II}% was increasing or decreasing, allowing for appropriate adjustment of i. Together, these results demonstrate that the Pt^{II}% can indeed be maintained over long time durations of catalysis through dynamically-controlled electrochemical oxidation.

Careful control of the Pt^{II}:Pt^{IV} ratio during the reaction is essential for another reason: Pt^{IV} ions suppress the irreversible decomposition of Pt^{II} to Pt^0.[9,16] Indeed, at the end of all of our EMOR trials, the bulk reaction solutions contained no visible Pt^0 precipitates. Only a few adventitious Pt^0 deposits were observed on the reactor surfaces and crevices where mass transport was restricted and replenishment of Pt^{IV} was impeded (see the SI, Section S5). One of the Pt^0 deposition mechanisms is disproportionation of Pt^{II}.[16] While the solution

DOI: 10.1021/acscentsci.9b00273
ACS Cent. Sci. 2019, 5, 1179−1186

composition is thermodynamically inclined to deposit Pt^0 (Figure S19),[41] our results demonstrate that, under sufficiently high [Pt^{IV}], nucleation of Pt^0 may be inhibited (see the SI, Section S5 and Table S3). Although an extensive discussion of Pt^0 deposition mechanisms is beyond the scope of the current work, these considerations highlight the importance of maintaining a stable Pt^{II}:Pt^{IV} ratio.

Analysis of Methane Oxidation Products from the EMOR Reactor. Operation of the EMOR reactor using the feedback modulation procedure described above allowed for continuous functionalization of methane (Table 1 and Figure 4). In all cases, we observe CH_3OH as the majority product in 69−72% yield (Table 1). We also observe appreciable quantities of CH_3Cl with a yield that decreases from 24% to 13% as the reaction time increases. Small amounts of overoxidized products ($CH_2(OH)_2$, HCOOH, and CO_2) were observed in less than 20% combined yield. Taking these overoxidized products to represent Pt^{II}-catalyzed oxidation of CH_3OH by 1, 2, and 3 equivalents of Pt^{IV}, respectively, the overall Faradaic efficiencies were in excess of 90% in all cases (Table S2). The per-Pt^{II} turnover numbers (TON) could not be rigorously determined due to minor fluctuations in [Pt^{II}] over the course of the reaction (see above), but approximate values were calculated from the known initial and final Pt^{II} amounts. For the longest trial, TON values of 6 and 9 for monofunctionalized products (CH_3X = CH_3OH and CH_3Cl) and total oxidation events were obtained, respectively (Table 1). The TOF for CH_3X, estimated to be 0.2−0.3 h^{-1}, showed a decreasing trend with increasing reaction time due to the overoxidation of CH_3OH. In contrast, the TOF for total oxidation events was relatively constant at ca. 0.3 h^{-1} for different reaction times. Together, these observations demonstrate that electrochemical reoxidation effectively sustains Pt^{II}-based methane functionalization catalysis.

Combining the four trials in Table 1, Figure 4a visualizes the temporal progression of EMOR. We fit these data to the set of reactions suggested earlier: oxidation of CH_4 to CH_3OH and CH_3Cl, hydrolysis of CH_3Cl to CH_3OH, and subsequent overoxidation of CH_3OH to $CH_2(OH)_2$, HCOOH, and CO_2 (Figure 4b). While the fitted apparent rate constants (Table S6) for $CH_2(OH)_2$ and HCOOH oxidation show deviation from values separately determined outside the reactor (Table S7), the fitted values for CH_4 and CH_3OH oxidation are in good agreement with those independent measurements (Table S8). Thus, this simple model provides a reasonable description of the methane oxidation processes taking place during the EMOR.

All of the EMOR experiments shown in Table 1 were performed with identical reaction solution compositions with a low (3 mM) catalyst concentration. When the concentrations of Pt^{II}, Pt^{IV}, and Cl^- were increased, CH_3OH and CH_3Cl output increased while the fraction of CO_2 decreased (see the SI, Section S6 and Table S5). These results suggest that there is ample room for optimization of the solution composition to maximize yield and selectivity.

Outlook for Practical Methane Oxidation. Our studies establish that electrochemical oxidation endows Shilov's catalyst with a sustainable mechanism for turnover and an inherent stability against deactivation through either complete oxidation of Pt^{II} to Pt^{IV} or Pt^0 deposition. However, we acknowledge that the Pt^{II} catalyst displays a relatively low reaction rate and moderate selectivity.[9] Our work does not directly address these inherent limitations of the catalyst; furthermore, our proof-of-concept reactor was not designed to demonstrate optimal TON, TOF, or selectivity for methanol. However, the EMOR approach developed here opens the door toward a broader exploration of reaction conditions and reactor configurations that may overcome these rate and selectivity limitations. For example, higher temperatures and catalyst concentrations could be employed to enhance the reaction rate, but these conditions would lower the kinetic barrier to deactivation by Pt^0 deposition. The EMOR can be used to maintain an optimal $Pt^{II/IV}$ ratio that is matched to these conditions (e.g., Figure S19, red square) and thereby sustain catalysis at higher volumetric productivity. Additionally, since the $Pt^{II}Cl_x(H_2O)_{(4-x)}^{(2-x)}$ catalyst displays modest selectivity for methane versus methanol oxidation (∼1:1) (SI, Table S8),[11] strategies for continuous product removal would be needed to minimize overoxidation. As opposed to a volatile chemical oxidant that may be released at a similar rate as the methanol product, electrochemical oxidation could allow for independent control of oxidant delivery and product release. While many challenges remain, EMOR offers new opportunities for developing practical Shilov-type systems for methane-to-methanol conversion.

Safety Statement. No unexpected or unusually high safety hazards were encountered.

CONCLUSIONS

We have established an electrochemical approach for continuous methane-to-methanol conversion using aqueous Pt^{II} catalysts. Cl-adsorbed Pt surfaces were shown to be competent for the inner-sphere two-electron oxidation of Pt^{II} to Pt^{IV} while inert toward parasitic oxidation of the methanol product. In situ potential measurements and current modulation allowed us to carry out continuous steady-state catalysis by maintaining the Pt^{II}:Pt^{IV} ratio. While our test reactors were run up to 30 h, further reactor engineering to automatically modulate the current in real-time, enhance solution mixing, and rigorously separate the anode and cathode compartments should allow for extended operation. Moreover, integration of an oxygen-consuming counter electrode will enable net aerobic methane-to-methanol conversion (eq 1). While many additional challenges remain to realize viable Pt^{II}-catalyzed methane conversion,[9] we envision that the electrochemical approach developed here will stimulate continued progress toward practical technologies for aerobic methane valorization.

ASSOCIATED CONTENT

Supporting Information

The Supporting Information is available free of charge on the ACS Publications website at DOI: 10.1021/acscentsci.9b00273.

Full experimental details, description of the high-temperature electrochemistry, additional electrochemical data, additional EMOR reactor data, electrolyte optimization, and substrate oxidation experiments (PDF)

AUTHOR INFORMATION

Corresponding Author

*E-mail: yogi@mit.edu.

DOI: 10.1021/acscentsci.9b00273
ACS Cent. Sci. 2019, 5, 1179−1186

ORCID

Yogesh Surendranath: 0000-0003-1016-3420

Notes

The authors declare the following competing financial interest(s): R.S.K. and Y.S. are inventors on provisional patent application 62/819,046 filed by the Massachusetts Institute of Technology that covers the electrochemical regeneration method reported in this work.

■ ACKNOWLEDGMENTS

We thank Travis Marshall-Roth, Patrick Smith, Michael Pegis, Thejas Wesley, Jaeyune Ryu, Bing Yan, Randall Field, and Sahag Voskian for helpful discussions. We thank Marcel Schreier and Jianbo Wang for assistance with GC analysis. This work was supported by Eni S.p.A. through the MIT Energy Initiative. Y.S. acknowledges the Sloan Foundation, Research Corporation for Science Advancement (Cottrell Scholar), and the Canadian Institute for Advanced Research (CIFAR Azrieli Global Scholar).

■ ABBREVIATIONS

EMOR, electrochemical methane oxidation reaction; FE, Faradaic efficiency; OCP, open-circuit potential; SHE, standard hydrogen electrode; FTO, fluorine-doped tin oxide; TON, turnover numbers; TOF, turnover frequencies

■ REFERENCES

(1) da Silva, M. J. Synthesis of Methanol from Methane: Challenges and Advances on the Multi-Step (Syngas) and One-Step Routes (DMTM). *Fuel Process. Technol.* **2016**, *145*, 42−61.

(2) Wang, B.; Albarracín-Suazo, S.; Pagan-Torres, Y.; Nikolla, E. Advances in Methane Conversion Processes. *Catal. Today* **2017**, *285*, 147−158.

(3) Olah, G. A. Beyond Oil and Gas: The Methanol Economy. *Angew. Chem., Int. Ed.* **2005**, *44*, 2636−2639.

(4) Holmen, A. Direct Conversion of Methane to Fuels and Chemicals. *Catal. Today* **2009**, *142*, 2−8.

(5) Bank, W. Zero Routine Flaring by 2030. www.worldbank.org/en/programs/zero-routine-flaring-by-2030 (accessed Sept 24, 2016).

(6) Promoppatum, P.; Viswanathan, V. Identifying Material and Device Targets for a Flare Gas Recovery System Utilizing Electrochemical Conversion of Methane to Methanol. *ACS Sustainable Chem. Eng.* **2016**, *4*, 1736−1745.

(7) Wogan, T. Methane to methanol catalyst could end gas flaring. www.chemistryworld.com/news/methane-to-methanol-catalyst-could-end-gas-flaring/3007247.article (accessed Feb 1, 2019).

(8) Ravi, M.; Ranocchiari, M.; van Bokhoven, J. A. The Direct Catalytic Oxidation of Methane to Methanol—A Critical Assessment. *Angew. Chem., Int. Ed.* **2017**, *56*, 16464−16483.

(9) Labinger, J. A.; Bercaw, J. E. Mechanistic Studies on the Shilov System: A Retrospective. *J. Organomet. Chem.* **2015**, *793*, 47−53.

(10) Latimer, A. A.; Kakekhani, A.; Kulkarni, A. R.; Nørskov, J. K. Direct Methane to Methanol: The Selectivity-Conversion Limit and Design Strategies. *ACS Catal.* **2018**, *8*, 6894−6907.

(11) Owen, J. S.; Labinger, J. A.; Bercaw, J. E. Kinetics and Mechanism of Methane, Methanol, and Dimethyl Ether C-H Activation with Electrophilic Platinum Complexes. *J. Am. Chem. Soc.* **2006**, *128*, 2005−2016.

(12) Labinger, J. A.; Bercaw, J. E.; Luinstra, G. A.; Lyon, D. K.; Herring, A. M. Organometallic Methane Activation: Functionalization by Aqueous Platinum Complexes. In. *Stud. Surf. Sci. Catal.* **1994**, *81*, 515−520.

(13) Michalkiewicz, B. Assessment of the Possibility of the Methane to Methanol Transformation. *Pol. J. Chem. Technol.* **2008**, *10*, 20−26.

(14) Labinger, J. A. Alkane Functionalization via Electrophilic Activation. In *Catalysis by Metal Complexes: Alkane C-H Activation by Single-Site Metal Catalysis*; Pérez, P. J., Ed.; Catalysis by Metal Complexes; Springer Netherlands: Dordrecht, 2012; Vol. *38*, Chapter 2, pp 17−71.

(15) Gunsalus, N. J.; Koppaka, A.; Park, S. H.; Bischof, S. M.; Hashiguchi, B. G.; Periana, R. A. Homogeneous Functionalization of Methane. *Chem. Rev.* **2017**, *117*, 8521−8573.

(16) DeVries, N.; Roe, D. C.; Thorn, D. L. Catalytic Hydroxylation Using Chloroplatinum Compounds. *J. Mol. Catal. A: Chem.* **2002**, *189*, 17−22.

(17) Weinberg, D. R.; Labinger, J. A.; Bercaw, J. E. Competitive Oxidation and Protonation of Aqueous Monomethylplatinum(II) Complexes: A Comparison of Oxidants. *Organometallics* **2007**, *26*, 167−172.

(18) Lin, M.; Shen, C.; Garcia-Zayas, E. A.; Sen, A. Catalytic Shilov Chemistry: Platinum Chloride-Catalyzed Oxidation of Terminal Methyl Groups by Dioxygen. *J. Am. Chem. Soc.* **2001**, *123*, 1000−1001.

(19) Bar-Nahum, I.; Khenkin, A. M.; Neumann, R. Mild, Aqueous, Aerobic, Catalytic Oxidation of Methane to Methanol and Acetaldehyde Catalyzed by a Supported Bipyrimidinylplatinum-Polyoxometalate Hybrid Compound. *J. Am. Chem. Soc.* **2004**, *126*, 10236−10237.

(20) Kreutz, J. E.; Shukhaev, A.; Du, W.; Druskin, S.; Daugulis, O.; Ismagilov, R. F. Evolution of Catalysts Directed by Genetic Algorithms in a Plug-Based Microfluidic Device Tested with Oxidation of Methane by Oxygen. *J. Am. Chem. Soc.* **2010**, *132*, 3128−3132.

(21) Lee, M.; Sanford, M. S. Platinum-Catalyzed, Terminal-Selective C(sp3)-H Oxidation of Aliphatic Amines. *J. Am. Chem. Soc.* **2015**, *137*, 12796−12799.

(22) Horváth, I. T.; Cook, R. A.; Millar, J. M.; Kiss, G. Low-Temperature Methane Chlorination with Aqueous Platinum Chlorides in the Presence of Chlorine. *Organometallics* **1993**, *12*, 8−10.

(23) Liu, S. F.; Nusrat, F. Electrocatalytic Shilov Chemistry for the Oxidation of Aliphatic Groups. *Mol. Catal.* **2019**, *463*, 16−19.

(24) Freund, M. S.; Labinger, J. A.; Lewis, N. S.; Bercaw, J. E. Electrocatalytic Functionalization of Alkanes Using Aqueous Platinum Salts. *J. Mol. Catal.* **1994**, *87*, L11−L15.

(25) Lappin, G. *Redox Mechanisms in Inorganic Chemistry*; Ellis Horwood: New York, 1994.

(26) Jude, H.; Krause Bauer, J. A.; Connick, W. B. An Outer-Sphere Two-Electron Platinum Reagent. *J. Am. Chem. Soc.* **2003**, *125*, 3446−3447.

(27) O'Reilly, M. E.; Kim, R. S.; Oh, S.; Surendranath, Y. Catalytic Methane Monofunctionalization by an Electrogenerated High-Valent Pd Intermediate. *ACS Cent. Sci.* **2017**, *3*, 1174−1179.

(28) Cushing, J. P.; Hubbard, A. T. Study of the Kinetics of Electrochemical Reactions By Thin Layer Voltammetry. II. Electro-Oxidation of Platinum (II) Complexes. *J. Electroanal. Chem. Interfacial Electrochem.* **1969**, *23*, 183−203.

(29) Vanysek, P. Thermo, Electro & Solution Chemistry: Electrochemical Series. In *CRC Handbook of Physics and Chemistry*, 99th ed.; CRC Press, 2018.

(30) Elding, L. I. Preparation and Properties of the Tetra-Aquaplatinum(II) Ion in Perchloric Acid Solution. *Inorg. Chim. Acta* **1976**, *20*, 65−69.

(31) Scortichini, C. L.; Reilley, C. N. Surface Characterization of Pt Electrodes Using Underpotential Deposition of H and Cu. V. Characterization of BD Pt Catalyst Surface. *J. Catal.* **1983**, *79*, 138−146.

(32) Jerkiewicz, G.; Vatankhah, G.; Lessard, J.; Soriaga, M. P.; Park, Y. S. Surface-Oxide Growth at Platinum Electrodes in Aqueous H2SO4 Reexamination of Its Mechanism through Combined Cyclic-Voltammetry, Electrochemical Quartz-Crystal Nanobalance, and Auger Electron Spectroscopy Measurements. *Electrochim. Acta* **2004**, *49*, 1451−1459.

(33) Novak, D. M.; Conway, B. E. Competitive Adsorption and State of Charge of Halide Ions in Monolayer Oxide Film Growth

DOI: 10.1021/acscentsci.9b00273
ACS Cent. Sci. 2019, 5, 1179−1186

Processes at Pt Anodes. *J. Chem. Soc., Faraday Trans. 1* **1981**, *77*, 2341−2359.
(34) Balashova, N. A.; Kazarinov, V. E. Study of the Structure of the Electrical Double Layer on Platinum by the Radioactive Tracer Method. *Russ. Chem. Rev.* **1965**, *34*, 730−736.
(35) Compton, R. G.; Banks, C. E. *Understanding Voltammetry*, 2nd ed.; World Scientific Publishing: Singapore, 2007.
(36) Zhao, X.; Yin, M.; Ma, L.; Liang, L.; Liu, C.; Liao, J.; Lu, T.; Xing, W. Recent Advances in Catalysts for Direct Methanol Fuel Cells. *Energy Environ. Sci.* **2011**, *4*, 2736.
(37) Chung, D. Y.; Lee, K. J.; Sung, Y. E. Methanol Electro-Oxidation on the Pt Surface: Revisiting the Cyclic Voltammetry Interpretation. *J. Phys. Chem. C* **2016**, *120*, 9028−9035.
(38) Snell, K. D.; Keenan, A. G. Chloride Inhibition of Ethanol Electrooxidation at a Platinum Electrode in Aqueous Acid Solution. *Electrochim. Acta* **1981**, *26*, 1339−1344.
(39) Sen, A.; Lin, M.; Kao, L. C.; Hutson, A. C. C-H Activation in Aqueous Medium. The Diverse Roles of Platinum(II) and Metallic Platinum in the Catalytic and Stoichiometric Oxidative Functionalization of Organic Substrates Including Alkanes. *J. Am. Chem. Soc.* **1992**, *114*, 6385−6392.
(40) Cardoso, D. S. P.; Šljukić, B.; Santos, D. M. F.; Sequeira, C. A. C. Organic Electrosynthesis: From Laboratorial Practice to Industrial Applications. *Org. Process Res. Dev.* **2017**, *21*, 1213−1226.
(41) Gammons, C. H. Experimental Investigations of the Hydrothermal Geochemistry of Platinum and Palladium: V. Equilibria between Platinum Metal, Pt(II), and Pt(IV) Chloride Complexes at 25 to 300°C. *Geochim. Cosmochim. Acta* **1996**, *60*, 1683−1694.

DOI: 10.1021/acscentsci.9b00273
ACS Cent. Sci. 2019, 5, 1179−1186